Intermetallics 88 (2017) 1–5

Contents lists available at ScienceDirect

Intermetallics

journal homepage: www.elsevier.com/locate/intermet

Unusual volume change associated with crystallization in Ce-Ga-Cu bulk metallic glass

Y. Zhao[a,b], B. Zhang[a,*], K. Sato[b,**]

[a] Institute of Amorphous Matter Science, School of Materials Science and Engineering & Anhui Provincial Key Lab of Advanced Functional Materials and Devices, Hefei University of Technology, Hefei 230009, China

[b] Department of Environmental Sciences, Tokyo Gakugei University, 4-1-1 Koganei, Tokyo 184-8501, Japan

ARTICLE INFO

Keywords:
Bulk metallic glass
Volume expansion
Crystallization
Dilatometry
Positron annihilation

ABSTRACT

In the general concept of crystallization kinetics, the amorphous solid with a number of open spaces transforms into a thermodynamically stable crystal, being denser than the corresponding amorphous phase. However, we unambiguously show that $Ce_{70}Ga_6Cu_{24}$ bulk metallic glass (BMG) exhibits volume expansion together with the density decrease upon crystallization in sharp contrast to other amorphous materials. This anomalous behavior is found to be explained by the formation of structurally loose interfaces among crystallites in the crystalline $Ce_{70}Ga_6Cu_{24}$ in addition to the disappearance of Ce-concentrated densely-packed local structure originally located in the amorphous matrix of BMG.

1. Introduction

Amorphous solids, as e.g., metallic glass, amorphous ceramic, inorganic glass, and polymer, are aperiodic materials that exhibit a random configuration of constituent atoms in the three-dimensional space [1–4]. In principle, the amorphous solids frozen from the high temperature melts exhibit metastable structures characteristic of excess free volume comparing with their corresponding crystal counterparts [5–7]. The amorphous solids thus become the interstitial structure with excess free volumes, which has been evidenced from the results of differential scanning calorimetry (DSC) [8–11], volume-change measurement using dilatometry (DLT) [12–14], and direct probing with positrons [15–18]. On moderately cooling, the liquid phase transforms into a thermodynamically stable crystal without free volumes, being denser than the amorphous state. This is the general concept of crystallization occurring in the amorphous solids, which is well documented in textbooks [19,20].

It has been however reported unusual volume expansion along with the density decrease upon crystallization for two alloy systems of BMG. The first alloy system is $Pd_{40}Ni_{40-x}Cu_xP_{20}$ BMGs, in which the molar volumes of the amorphous state are lower than those of corresponding crystals in the composition rage $x > 30$ [21]. The second system is $Zr_{52.5}Cu_{17.9}Ni_{14.6}Al_{10}Ti_5$ BMG produced using high purity raw materials suppressing the oxygen concentration [22]. The above findings dependent on a chemical composition as well as a purity imply a certain resistivity against crystallization, thus stimulating a fundamental interest in how an excellent glass-forming ability emerges together with the densely agglomerated atomic structure in the amorphous matrix of BMGs. In this work, both the volume and density changes caused by crystallization are explored for $Ce_{70}Ga_6Cu_{24}$ BMG. We first study the crystallization behavior of BMG by density measurement with the Archimedes method, ex situ and in situ X-ray diffraction (XRD), and length-change measurement using DLT. And then, the atomistic mechanism of crystallization-induced volume and density changes is highlighted on the basis of local atomic sites probed by element-specific positron annihilation spectroscopy.

2. Experiments procedures

$Ce_{70}Ga_6Cu_{24}$ BMG rod with a diameter of 5 mm was prepared by a Cu-mold casting method in purified argon atmosphere. Thermal properties were examined by DSC under a purified nitrogen atmosphere in a PE 8000 system with a heating rate of 20 K/min. Glass transition temperature T_g and crystallization temperature T_x are 352 and 399 K, respectively. The crystalline $Ce_{70}Ga_6Cu_{24}$ was prepared by annealing at 573 K for 2 h in the vacuum of $\sim 3 \times 10^{-3}$ Pa. The oxygen contents in both glassy and crystalline samples were measured by X-ray photoelectron spectroscopy (XPS) technique in an Escalab 250 system (Thermo, USA). In order to make sure that the measured oxygen content is inside the sample rather than on the sample surface, a 10-min long time

* Corresponding author.
** Corresponding author.
E-mail addresses: bo.zhang@hfut.edu.cn (B. Zhang), sato-k@u-gakugei.ac.jp (K. Sato).

http://dx.doi.org/10.1016/j.intermet.2017.04.017
Received 15 February 2017; Received in revised form 25 March 2017; Accepted 22 April 2017

Table 1
Relative density (ρ), positron lifetimes (τ_1 and τ_2), the relative intensities of τ_1 and τ_2 (I_1 and I_2) for the crystalline $Ce_{70}Ga_6Cu_{24}$. The data of $Ce_{70}Ga_6Cu_{24}$ BMG were added for comparison [23,24]. Positron lifetimes at defect-free (τ_f) and monovacancy (τ_{1v}) for several pure Ce, Ga, and Cu [25] are shown as well.

$Ce_{70}Ga_6Cu_{24}$	ρ [g cm^{-3}]	τ_1 [ps]	τ_2 [ps]	I_1 [%]	I_2 [%]
crystal	6.851	159	284	17	83
BMG [23,24]	6.972	130	261	28	72
Pure metal		τ_f [ps]	τ_{1v} [ps]		
Ce [25]		197	315		
Ga [25]		165	238		
Cu [25]		105	178		

etching procedure by Argon ion was performed to remove the surface oxidation layer of the sample just before XPS measurement. Relative densities ρ measurements were carried out by using Archimedes method with sample weights larger than 1.0 g and the measuring uncertainties are within 0.2%. Densities ρ for the amorphous [23] and crystalline $Ce_{70}Ga_6Cu_{24}$ are 6.972 and 6.851 g cm^{-3}, respectively (see Table 1). Note that the crystalline $Ce_{70}Ga_6Cu_{24}$ has lower density than that of the corresponding BMG.

Ex situ and in situ XRD studies were performed for the $Ce_{70}Ga_6Cu_{24}$ BMG using diffractometer with Cu *K*α radiation (XRD, Ultima IV, RIGAKU). Time-resolved in situ XRD patterns were obtained after up quenching to 357 K (above T_g) at a heating rate of 1 K/min. Length-change measurements were performed for the $Ce_{70}Ga_6Cu_{24}$ BMG with a high-precision differential-type dilatometer (TD5020SA, Bruker AXS) equipped with a closed-water-cycling system [14]. Time-resolved length-change data were obtained after up quenching to the target temperatures at a heating rate of 1 K/min. For the positron lifetime and coincident Doppler broadening (CDB) [26,27] spectroscopy experiments, the crystalline $Ce_{70}Ga_6Cu_{24}$ sample was cut into two identical disks with a thickness of 2 mm. The positron source (^{22}Na), sealed in a thin foil of Kapton, was mounted in a sample-source-sample sandwich for the measurements. Positron lifetime spectra ($\sim 1 \times 10^6$ coincidence counts) were recorded with digital oscilloscope-based system, in which the time resolution of 190 ps full-width at half-maximum (FWHM) was achieved. The positron lifetime spectrum was numerically analyzed using the POSITRONFIT code [28]. In CDB spectroscopy, the energies of the two annihilation quanta E_1 and E_2 were measured with a collinear set-up of two high-purity Ge detectors. The spectra were obtained by cutting the E_1, E_2 spectra along the energy conservation line $E_1 + E_2 = (1022 \pm 1)$ keV, taking into account the annihilation events within a strip of ± 1.6 keV.

3. Results and discussion

Fig. 1(a) shows ex situ XRD patterns for the $Ce_{70}Ga_6Cu_{24}$ BMG without annealing, annealed at 372 K (above T_g) for 7 h, at 573 K (above T_x) for 2 h, and at 499 K (above T_x) for 40 h. The diffraction pattern exhibits a broad hallo indicating a typical amorphous structure for the BMG sample. XRD peaks arising from the crystalline Ce_5Ga_3 phase begin to appear together with that from the γ-Ce phase for the sample annealed at 372 K for 7 h. On annealing at 499 K for 40 h, the XRD peaks of the Ce_5Ga_3 and γ-Ce phases disappear and other peaks of crystalline phases such as Ce_3Ga and Cu in turn appear. On annealing at 573 K for 2 h, the XRD pattern is very similar to that of the sample annealed at 499 K for 40 h except that very small part of Ce_5Ga_3 phase persists. In Fig. 1(b) shows the XRD pattern for the sample annealed at 347 K (below T_g) for 300 h, in which the XRD peaks arising from not the γ-Ce phase but the Ce_5Ga_3 one are observed. This indicates that the Ce_5Ga_3 phase is formed earlier than that of γ-Ce phase in the crystallization process.

Fig. 2 shows the results of in situ XRD for the $Ce_{70}Ga_6Cu_{24}$ BMG, where the time-dependent structural evolution occurring at 357 K

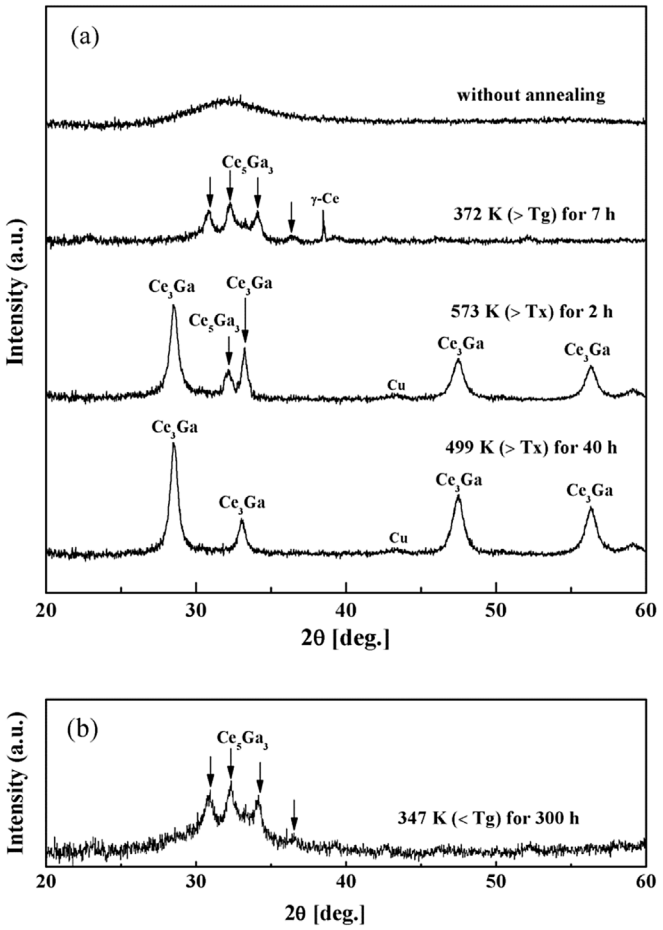

Fig. 1. Ex situ XRD patterns for $Ce_{70}Ga_6Cu_{24}$ BMG (a) without annealing, annealed at 372 K (above T_g) for 7 h, at 573 K (above T_x) for 2 h, and at 499 K (above T_x) for 40 h, and (b) annealed at 347 K (below T_g) for 300 h.

(above T_g) is well seen. The XRD pattern exhibits a typical amorphous structure prior to annealing. An onset of Ce_5Ga_3 crystallization is clearly visible when the BMG sample is annealed for 1 h, in consistent with the results of ex situ XRD. In addition to the Ce_5Ga_3 phase, the XRD peak arising from the CeCu phase appears here. With increasing the annealing time up to 3 h, the above onset peaks are significantly sharpened and the peak of γ-Ce phase appears as well similarly to the results of ex situ XRD. The results of in situ XRD sequentially observed here provide the further additional information on the crystallization process that the CeCu phase is formed earlier than that of γ-Ce. The diffraction patterns are completely changed at 10 h, where the peaks of Ce_5Ga_3, CeCu, and γ-Ce phases disappear and Ce_3Ga alternatively appears. This is in agreement with the ex situ XRD pattern observed at 499 K higher than T_x.

It is noted that cubic CeO_2 has a lattice parameter of 5.41 Å and shows similar XRD pattern with that of Ce_3Ga phase. So it is necessary to make sure that the XRD patterns arise from Ce_3Ga rather than CeO_2. According to oxygen content results measured by XPS, 0.98 and 1.03 wt % oxygen was detected in the glassy and crystalline $Ce_{70}Ga_6Cu_{24}$ sample, respectively. The oxygen content is much lower than that of Ga content, so the Ce_3Ga phase is more dominant than CeO_2 in the sample. CeO_2 is easy to be formed in the sample surface with nm-dimension, which is much lower than the penetration depth of X-ray with Cu-*K* radiation with μm-dimension. Thus it is believed that crystallized XRD patterns arise from Ce_3Ga phase rather than CeO_2.

Based on the combined results of ex situ and in situ XRD studies, the following two-step crystallization mechanism can be drawn for the $Ce_{70}Ga_6Cu_{24}$ BMG. The 1st step begins with an onset of crystallization